Preparation of Nitrogen-containing Activated Carbon from Waste Medium Density Fiberboard for Electric Double Layer Capacitor

Xiaoxu Cai, Ruquan Ren, Mingyang Zhang, Xiaojuan Jin,* and Qiang Zhao

The waste of medium density fiberboards was carbonized at a temperature of 500 °C. The activated carbons were obtained after 16 h of impregnation and 1 h of activation by KOH at 800 °C with KOH/coke mass ratios of 2.5, 3.0, 3.5, and 4.0. The activated carbons were investigated for determination of porosity and elemental analysis. The results showed that the surface area of the activated carbons varied from 1456 to 1647 m^2/g and the total pore volume ranged from 0.701 to 1.106 cm^3/g, which was affected by different KOH/coke mass ratios. The pore size distribution indicated that waste medium density fiberboard activated carbons included both micropores and mesopores, and the elemental analysis implied that the contents of nitrogen varied from 0.97% to 2.60%. Electric double layer capacitors were made using the activated carbons and their electrochemical properties were studied. The specific capacitances of the activated carbon electrodes ranged from 212 to 223 F/g. The results suggest that activated carbon from waste medium density fiberboard can be a candidate material for electric double layer capacitor electrodes because of its good electrochemical capacities.

Keywords: Electrochemical properties; Nitrogen-containing activated carbon; KOH activation; Waste medium density fiberboard

*Contact information: MOE Key Laboratory of Wooden Material Science and Application, Beijing Key Laboratory of Lignocellulosic Chemistry, MOE Engineering Research Center of Forestry Biomass Materials and Bioenergy Beijing Forestry University 35 Qinghua East road, Haidian, 100083, Beijing, China; *Corresponding author: jxj0322@163.com*

INTRODUCTION

Electric double layer capacitors (EDLCs), also known as electrochemical capacitors (ECs) or supercapacitors, are a kind of energy-storage device characterized by excellent rate capability and long cyclic life compared to secondary batteries and are applicable in electric vehicles, portable consumer electronics, uninterrupted power sources, memory backup, and much more (Frackowiak and Beguin 2001; Winter and Brodd 2004; Arico *et al.* 2005; Wang *et al.* 2012). Recently, numerous efforts have been devoted to exploring optimum EDLC electrode materials. Various carbon materials, such as activated carbon, carbon nanotubes, graphene, carbon aerogels, and carbon nanofibers, have been studied from the viewpoint of both capacitive and electrocatalytic properties (Vujković *et al.* 2013). Of these materials, activated carbon (AC) has attracted much attention because of its low cost, abundance, good mechanical strength, and high surface area (Dipali *et al.* 2014).

Many authors have correlated the capacitance with textural characteristics (specific surface area and pore size distribution) of carbon materials to determine whether the microporosity, mesoporosity, or their particular balance affect the double-layer

behavior. Apart from the textural effects, it is widely accepted that the presence and distribution of N- and O-containing groups on the carbon surface also influence the capacitor performance (Vujković *et al.* 2013). N- and O-containing groups can considerably enhance the total specific capacitances. Especially, nitrogen on the carbon skeleton not only can provide great pseudocapacitance but also improve the wettability of the as-prepared material in the electrolyte and thus can increase the surface utilization. Additionally, N doping was also found to enhance the electronic conductivity of the carbon material itself, favoring enhanced power properties (Hou *et al.* 2013). Four nitrogen species commonly exist in nitrogen-containing carbon, including pyridinic nitrogen (N-6), pyrrolic nitrogen (N-5), quarternary nitrogen (N-Q), and pyridine-N-oxide (N-X) (Chen *et al.* 2013). According to many previous studies (Zhang *et al.* 2012; Shang *et al.* 2015), nitrogen located at the edges of graphene layers, that is N-6 and N-5, are considered to be responsible for the pseudocapacitance effect.

In general, two strategies are applied to incorporate N species into mesoporous carbon materials. One strategy is post-treatment of carbon materials with ammonia, amine, or urea to introduce N-containing functional groups on their surfaces; unfortunately, this cannot change the bulk properties of the carbon materials (Hulicova-Jurcakova *et al.* 2009; Wu *et al.* 2012). The other strategy is *in situ* doping using various N-containing precursors, including melamine resin (Li *et al.* 2007, a), polyaniline (PANI) (Li *et al.* 2007b; Mentus *et al.* 2009; Trchová *et al.* 2009; Kim *et al.* 2010; Yang *et al.* 2010; Yin *et al.* 2010; Gavrilov *et al.* 2011, 2012; Janošević *et al.* 2011, 2012; Yuan *et al.* 2011), or polyacrylonitrile (Ra *et al.* 2009), to make a more homogeneous incorporation of the N species into the carbons with controlled chemistry; however the cost of N-containing precursors is high. In this study, waste medium density fiberboard (MDF) was used to reduce the cost. In the waste MDF, nitrogen was provided by the adhesive. The adhesives were urea-formaldehyde and melamine-formaldehyde resins, dispersed all through the board and impregnating each particle of wood. Wu *et al.* (2013) suggested that the preparation of nitrogen-containing AC from waste MDF is possible.

In this study, nitrogen-containing activated carbons were produced from waste MDF by chemical activation with potassium hydroxide. Different KOH/coke mass ratios were applied to prepare a series of ACs. The effects of the KOH/coke mass ratio on the porosity and electrochemical properties were investigated.

EXPERIMENTAL

Preparation of AC

Waste MDF was collected from a furniture factory in Beijing, China. The MDF consisted of poplar and urea-formaldehyde resin (wt. 12%). Analytical-grade KOH was purchased from Beijing Lanyi Chemical Reagent. The elemental analysis of the raw material, named C0, is shown in Table 2. The MDF was cut into pieces and then heated to a carbonization temperature of 500 °C at a heating rate of 100 °C/h and held at this temperature for 1 h. The samples were then ground and screened. The fraction in the particle diameter ranged from 40 to 60 mesh. The particle samples were dried in a 105 °C oven for 4 h, designated C500 for testing. In the activation step, the dried samples were mixed with 50% KOH solution with different impregnation ratios (KOH/coke mass ratios of 2.5:1, 3:1, 3.5:1, and 4:1) for 16 h. The mixtures were then dried in an electric stove, followed by activation in an electric furnace under nitrogen flow at

800 °C for 1 h. After cooling under nitrogen flow, the activated resultant was boiled with HCl and thoroughly washed with distilled water until the pH value of the filtrate became neutral. Finally, the samples were dried in a 105 °C oven for 4 h. The ACs were designated AC-X, where X represents the impregnation ratio, *i.e.*, AC-2.5, AC-3, AC-3.5, and AC-4.

Preparation of Electrode

The dried AC samples were ground in an agate mortar. These samples were then mixed with acetylene black and 60% polytetrafluoroethylene at a mass ratio of 87:10:3. The mixtures were sandwiched by nickel foam (square, about 1 cm^2) and pressed under a pressure of 20 MPa with a nickel tape for connection to one disk (Jiang *et al.* 2009) to obtain the electrodes.

Characterization of AC and Electrochemical Measurements

The pore structure characteristics of the ACs were measured by N_2 adsorption / desorption isotherms at 77 K. BET surface area was calculated from the N_2 adsorption / desorption isotherms using the Brunauer-Emmett-Teller (BET) equation (Gregg and Sing 1982). The N_2 adsorption–desorption isotherms of activated carbon prepared under optimum conditions were measured with an accelerated surface area in a porosimetry system (ASAP 2010, Micromeritics) for determining the surface areas. For the mesopore surface area, pore volume, and pore diameter, the Barrett-Joyner-Halenda (BJH) method was used. Micropore surface area and pore volume were determined using the t-method, and the micropore diameter was determined using the Dubinin-Astakhov (DA) method. The elemental analysis (carbon, hydrogen, and nitrogen) of the ACs was carried out in an elemental analyzer under a N_2 flow rate of 201 mL/min. In addition, the chemical composition and state of the ACs were determined by X-ray photoelectron spectroscopy (XPS) with an ESCALAB 250 instrument (VG Scientific, UK).

Electrochemical characteristics were tested in a 7 M KOH solution from 0 to 1 V at 50 mA/g. The constant current density charge-discharge and rate performance were tested by a BT2000 battery testing system (Arbin Instruments, USA) at room temperature. Specific capacitances of the activated carbon electrodes are expressed in F/g, as calculated using Eq. 1,

$$C_g = \frac{2i\Delta t}{ma\Delta V} \quad (1)$$

where i is current density discharge, Δt is the increment of time, m is the average quality of a single electrode, a is the mass fraction of the electrode activated section, and ΔV is the electric potential difference during discharging.

Cyclic voltammetry (CV) and alternating current impedance were employed in each sample for the electrochemical measurements using a 1260 electrochemical workstation (Solartron Metrology, UK) at room temperature. The gravimetric capacitance (C_p), which is the specific capacitance *per* mass weight of activated carbon in the electrode, is expressed in F/g and calculated using Eqs. 2 and 3 (Zhang *et al.* 2013),

$$C = \frac{Q}{U} = \frac{Q}{t} \times \frac{t}{U} = I \times \frac{t}{U} = \frac{I}{U/t} \quad (2)$$

$$C_p = \frac{C}{m} = \frac{I/m}{U/t} = \frac{I/m}{v} \quad (3)$$

where I is the observed value, m is the average weight of activated carbon disks, and v is the voltage scan rate.

RESULTS AND DISCUSSION

Characterization of ACs

Figure 1 shows the N_2 adsorption-desorption isotherms of the ACs from MDF. All ACs showed almost flat plateaus at higher relative pressures, typical of a type 1 isotherm. The small hysteresis loops seen on the adsorption-desorption isotherms were due to the existence of mesopores (Guo and Rockstraw 2007). When the KOH/coke mass ratio was increased, the adsorption capacity was increased correspondingly. Furthermore, the adsorption capacity of AC-3 was close to that of AC-3.5. The same result is shown in Table 1.

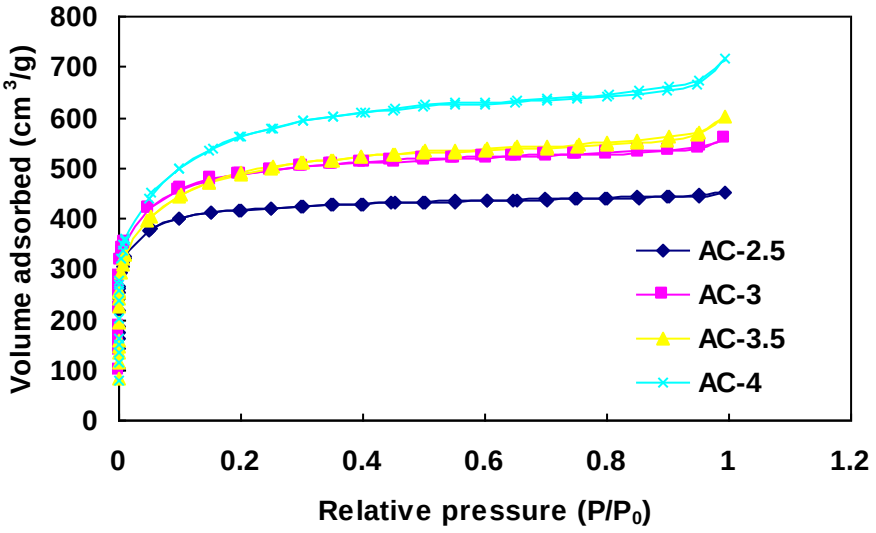

Fig. 1. N_2 adsorption-desorption isotherms for ACs prepared at various impregnation ratios

Table 1. Structural Characteristics of the Activated Carbons with Different Impregnation Ratios

KOH/coke	S_{BET} (m^2/g)	S_{me} (m^2/g)	S_{mi} (m^2/g)	V_{tot} (cm^3/g)	V_{mi} (cm^3/g)	V_{me} (cm^3/g)
2.5(AC-2.5)	1456	32	1404	0.701	0.634	0.561
3(AC-3)	1502	55	1404	0.862	0.737	0.106
3.5(AC-3.5)	1598	59	1377	0.931	0.736	0.155
4(AC-4)	1647	103	1486	1.106	0.853	0.222

S_{BET}: surface areas; S_{me}: mesopore area; S_{mi}: micropore area; V_{tot}: total pore volumes; V_{mi}: micropore volumes; V_{me}: mesopore volumes

Table 1 lists the physical properties of the ACs. As the impregnation ratio increased from 2.5 to 4, the BET surface area and pore volume of the mesopores increased. The BET surface area of the samples covered a narrow range from 1456 to 1647 m^2/g. The maximum BET surface area of 1647 m^2/g and mesopore volume of 0.222 cm^3/g were obtained for AC-4.

Table 2 lists the elemental data for all the samples. The carbon content increased after carbonization, but the nitrogen and hydrogen contents decreased. Activation with KOH resulted in higher contents of C, but lower contents of H and N than in the raw material. Furthermore, the contents of N and C had a downtrend with increasing impregnation ratio, and the H content increased gradually. N was present at levels ranging typically from 0.97 to 2.60%. This indicates that nitrogen-containing activated carbon could be obtained from waste MDF using KOH.

Table 2. Elemental Analysis of the ACs

	Composition (wt%)		
Sample	N (%)	C (%)	H (%)
C0	8.39	45.16	5.76
C500	6.81	74.50	2.69
AC-2.5	2.60	69.32	0.86
AC-3	2.09	60.96	1.73
AC-3.5	1.57	60.75	1.09
AC-4	0.97	58.80	1.10

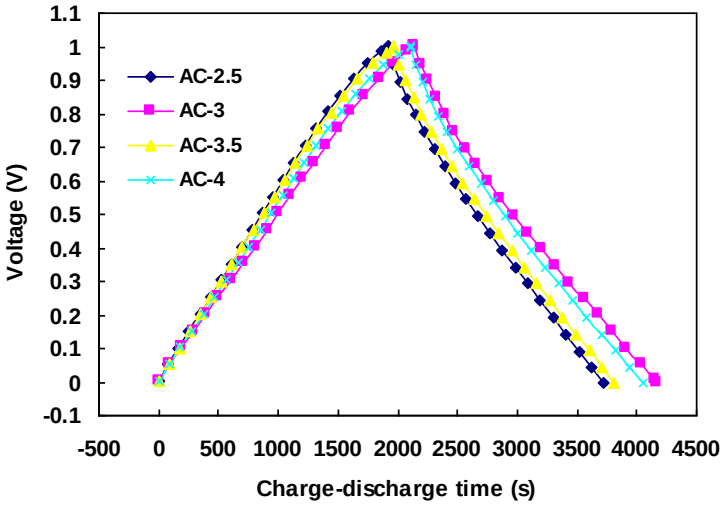

Fig. 2. Constant current density charge-discharge curves for AC capacitors

Electrochemical Performance of Activated Carbon Electrodes

Figure 2 shows the constant current charge-discharge curves for AC-2.5, AC-3, AC-3.5, and AC-4 electrodes using a 7 M KOH solution as the electrolyte at 50 mA/g current density (9th cycle) as an example. The shape of the curve for all samples was triangular, which confirmed the ideal capacitive behavior of the material with almost symmetric charge/discharge curves.

Figure 3 illustrates the specific capacitance of the different AC electrodes at various current densities (1st cycle). The specific capacitance of the AC electrodes ranged from 212 to 223 F/g at 0.05 A/g, and the specific capacitance had a downtrend in a narrow range of 0.5 to 10 A/g, especially when the KOH/coke ratio was 3. The specific capacitance of AC-3 was greater than that of AC-2.5, AC-3.5, and AC-4. The BET surface area of AC-3 was only 1502 m^2/g, which was less than that of AC-3.5 and AC-4 from Table 1; however, the content of N was 2.09%, which was greater than that of AC-3.5 and AC-4, as shown in Table 2. The results indicate that ACs containing N electrode materials possessed larger specific capacitances.

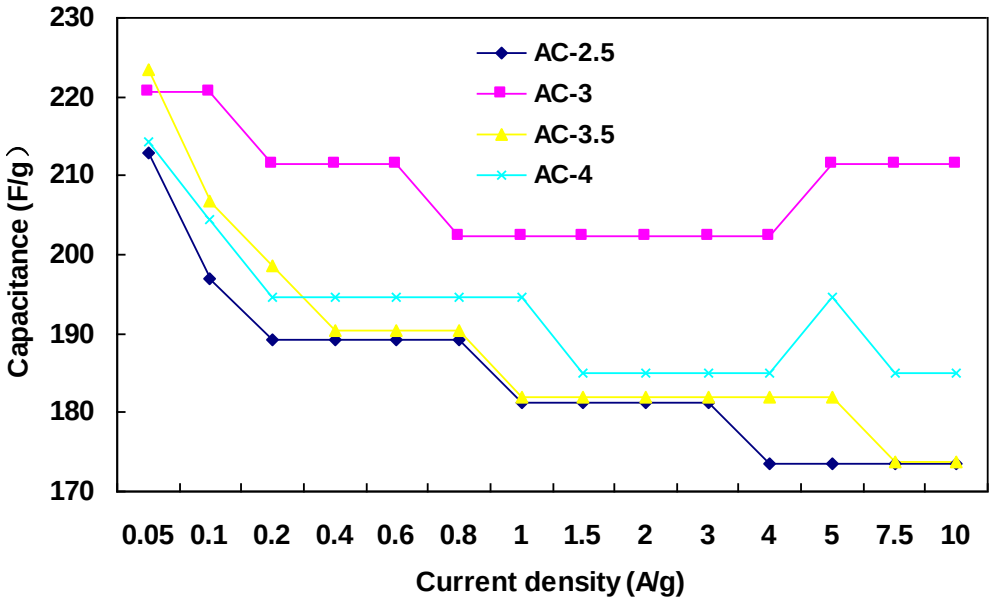

Fig. 3. Rate performances of AC capacitors

Figure 4 shows the CV curves of the AC-3 electrode between 0 and 1 V at different scan rates (2 mV/s, 10 mV/s, 20 mV/s, 50 mV/s, and 100 mV/s). The CV curves were very similar in shape, resembling a rectangle. The asymmetry of the CV curves with respect to the potential axis has been attributed elsewhere to the pseudo-Faradaic processes on the surface involving surface nitrogen (Moreno-Castilla *et al.* 2012). The hump during the sweep within the range 0.8 to 1.0 V has been usually attributed to pseudo-Faradaic reactions involving the nitrogen functional groups (Shang *et al.* 2014).

The Nyquist plot, which comes from a methodology known as electrochemical impedance spectroscopy (EIS), shows the frequency response of the electrode/electrolyte system and is a plot of the imaginary component of the impedance against the real component. The Nyquist plot toward the prepared carbons were measured and further fitted by Chi604d software, as shown in Fig. 5.

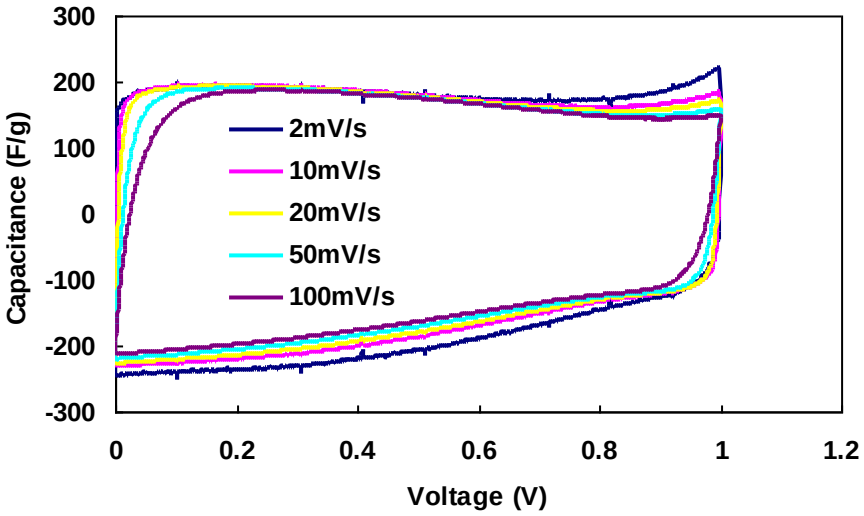

Fig. 4. Cyclic voltammograms of AC-3 capacitor at different sweep rates

A straight line in the low frequency region and a small arc in the high frequency region are typical behavior for a supercapacitor. At very high frequencies, the intercept at the real axis is the ESR (equivalent series resistance) value, and it can be seen that the ESR value of AC-3 was about 0.21. In the low frequency region the slope reflects the diffusive resistivity of the electrolyte ions within the pores, whereas AC-3 exhibits a near vertical line which indicates ideal capacitive behavior.

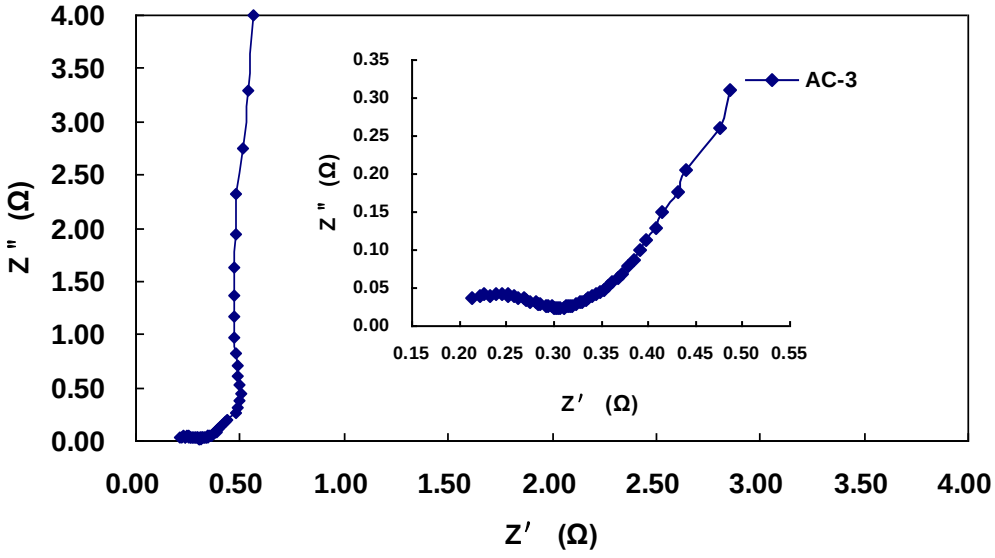

Fig. 5. Impedance spectrum of AC-3 capacitor at a sweep frequency of 0.01 Hz and control voltage of 1 V

From the results in Fig. 5 it is concluded that nitrogen-containing AC with high specific surface area from waste MDF and KOH can be a good material for preparation of EDLC electrodes.

CONCLUSIONS

Nitrogen-containing activated carbons (ACs) were prepared from waste medium density fiberboard and KOH. The effects of impregnation ratio on the porosity and elemental analysis of prepared ACs were investigated.

1. The surface area of the ACs ranged from 1456 to 1647 m^2 g^{-1}, and the total pore volume varied from 0.701 to 1.106 cm^3 g^{-1} as the impregnation ratio increased from 2.5:1 to 4:1.
2. The pore size distribution indicated that waste medium density fiberboard ACs included both micropores and mesopores.
3. The specific capacitances of the AC electrodes ranged from 212 to 223 F/g. These results suggest that waste MDF can be used to prepare EDLC electrode materials.

ACKNOWLEDGMENTS

The authors are greatly indebted to the State Forestry Administration under Project 201204807: The Study on the Technology and Mechanism of the Activated Carbon Electrode from Waste Hard Board. The authors also acknowledge funding from the project National Natural Science: The Chemistry Mechanism of Color System Forming during the Process of Wood Heat Inducing Discolor (31070490).

REFERENCES CITED

Arico, A. S., Bruce, P., Scrosati, B., Tarascon, J. M., and Schalkwijk, W. V. (2005). "Nanostructured materials for advanced energy conversion and storage devices," *Nat. Mater.* 4(5), 366-377. DOI: 10.1038/nmat1368

Chen, X. Y., Chen, C., Zhang, Z. J., Xie, D. H., Deng, X., and Liu, J. W. (2013). "Nitrogen-doped porous carbon for supercapacitor with long-term electrochemical stability," *Journal of Power Sources* 230, 50-58.

Frackowiak, E., and Beguin, F. (2001). "Carbon materials for electrochemical storage of energy in capacitors," *Carbon* 39(6), 937-950.

Gavrilov, N., Vujković, M., Pašti, I. A., Círić-Marjanović, G., and Mentus, S. V. (2011). "Enhancement of electrocatalytic properties of carbonized polyaniline nanoparticles upon a hydrothermal treatment in alkaline medium," *Electrochim. Acta* 56(25), 9197-9202. DOI: 10.1016/j.electacta.2011.07.134

Gavrilov, N., Pašti, I. A., Vujković, M., Travas-Sejdic, J., Círić-Marjanović, G., and Mentus, S. V. (2012). "High-performance charge storage by N-containing nanostructured carbon derived from polyaniline," *Carbon* 50(10), 3915-3927. DOI: 10.1016/j.carbon.2012.04.045

Gregg, S. J., and Sing, K. S. W. (1982). *Adsorption, Surface Area and Porosity*, Academic Press, New York.

Guo, Y., and Rockstraw, D. A. (2007). "Activated carbons prepared from rice hull by one-step phosphoric acid activation," *Micropor. Mesopor. Mater.* 100(1-3), 12-19. DOI: 10.1016/j.micromeso.2006.10.006

Hou, L. R., Lian, L., Li, D. K., Pang, G., Li, J. F., Zhang, X. G., Xiong, S. L., and Yuan, C. Z. (2013). "Mesoporous N-containing carbon nanosheets towards high-performance electrochemical capacitors," *Carbon* 64, 141-149. DOI: 10.1016/j.carbon.2013.07.045

Hulicova-Jurcakova, D., Kodama, M., Shiraishhi, S., Hatori, H., Zhu, Z. H., and Lu, G. Q. (2009). "Nitrogen-enriched nonporous carbon electrodes with extraordinary supercapacitance," *Adv. Funct. Mater.* 19(11), 1800-1809. DOI: 10.1002/adfm.200801100

Janošević, A., Pašti, I., Gavrilov, N., Mentus, S., Ćirić-Marjanović, G., Krstić, J. and Stejskal, J. (2011). "Micro/mesoporous conducting carbonized polyaniline 5-sulfosalicylate nanorods/nanotubes: Synthesis, characterization and electrocatalysis," *Synth. Met.* 161(19-20), 2179-2184. DOI: 10.1016/j.synthmet.2011.08.028

Janošević, A., Pašti, I., Gavrilov, N., Mentus, S., Krstić, J., and Mitrić, M. (2012) "Microporous conducting carbonized polyaniline nanorods: Synthesis, characterization and electrocatalytic properties," *Micropor. Mesopor. Mater.* 152(50), 50-57. DOI: 10.1016/j.micromeso.2011.12.002

Jiang, J. H., Gao, Q. M., Xia, K. S., and Hu, J. (2009). "Enhanced electrical capacitance of porous carbons by nitrogen enrichment and control of the pore structure," *Micropor. Mesopor. Mater.* 118(1/3), 28-34. DOI: 10.1016/j.micromeso.2008.08.011

Kim, W., Kang, M. Y., Joo, J. B., Kim, N. D., Son, I. K., Kim, P., Yoon, J. R., and Yi, J. (2010). "Preparation of ordered mesoporous carbon nanopipes with controlled nitrogen species for application in electrical double-layer capacitors," *J. Power Sources* 195(7), 2125-2129. DOI: 10.1016/j.jpowsour.2009.09.080

Li, W. R., Chen, D. H., Li, Z., Shi, Y. F., Wan, Y., Wang, G., Jiang, Z. Y., and Zhao, D. Y. (2007a) "Nitrogen containing carbon spheres with large uniform mesopores: The superior electrode materials for EDLC in organic electrolyte," *Carbon* 45(9), 1757-1763. DOI: 10.1016/j.carbon.2007.05.004

Li, W. R., Chen, D. H., Li, Z., Shi, Y. F., Wan, Y., Huang, J. J., Yang, J. J., Zhao, D. Y. and Jiang Z. Y. (2007b). "Nitrogen enriched mesoporous carbon spheres obtained by a facile method and its application for electrochemical capacitor," *Electrochem. Comm.* 9(4), 569-573. DOI: 10.1016/j.elecom.2006.10.027

Mentus, S., Ćirić-Marjanović, G., Trchová, M., and Stejskal, J. (2009). "Conducting carbonized polyaniline nanotubes," *Nanotech.* 20(24), 245601. DOI: 10.1088/0957-4484/20/24/245601

Moreno-Castilla, C., Dawidzuik, M. B., Carrasco-Marin, F., and Morallon, E. (2012). "Electrochemical performance of carbon gels with variable surface chemistry and physics," *Carbon* 50(9), 3324-3332. DOI: 10.1016/j.carbon.2011.12.047

Ra, E. J., Raymundo-Piñero, E., Lee, Y. H., and Béguin, F. (2009). "High power supercapacitors using polyacrylonitrile-based carbon nanofiber paper," *Carbon* 47(13), 2984-2992. DOI: 10.1016/j.carbon.2009.06.051

Shang, T. X., Zhang, M. Y., and Jin, X. J. (2014). "Easy procedure to prepare nitrogen-containing activated carbons for supercapacitors," *RSC Advances* 4(73), 39037-39044.

Shang, T. X., Ren, R. Q., Zhu, Y. M., and Jin, X. J. (2015). "Oxygen- and nitrogen-co-doped activated carbon from waste particleboard for potential application in high-performance capacitance," *Electrochimica Acta* 163, 32-40.

Trchová, M., Konyushenko, N. E., Stejskal, J., Kovářová, J., and Ćirić-Marjanović, G. (2009). "The conversion of polyaniine nanotubes to nitrogen-containing carbon

nanotubes and their comparison with multi-walled carbon nanotubes," *Polym. Degrad. Stab.* 94(6), 929-938.

Vujković, M., Gavrilov, N., Pašti, I., Krstić, J., Travas-Sejdic, J., Ćirić-Marjanovic, G. and Mentus, S. (2013). "Superior capacitive and electrocatalytic properties of carbonized nanostructured polyaniline upon a low-temperature hydrothermal treatment," *Carbon* 64, 472-486. DOI: 10.1016/j.carbon.2013.07.100

Wang, G. P., Zhang, L., and Zhang, J. J. (2012). "A review of electrode materials for electrochemical supercapacitors," *Chem. Soc. Rev.* 41(2), 797-828.

Winter, M., and Brodd, R. J. (2004). "What are batteries, fuel cells and supercapacitors," *Chem. Rev.* 104(10), 4245-4269. DOI: 10.1021/cr020730k

Wu, Z. X., Webley, P. A., and Zhao, D. Y. (2012). "Post-enrichment of nitrogen in soft-templated ordered mesoporous carbon materials for highly efficient phenol removal and CO_2 capture," *J. Mater. Chem.* 22(22), 11379-11389. DOI: 10.1039/c2jm16183d

Wu, Y., Jin, X. J., and Zhang, J. (2013). "Characteristics of nitrogen-enriched activated carbon prepared from waste medium density fiberboard by potassium hydroxide," *J. Wood Sci.* 59(2), 133-140. DOI: 10.1007/s10086-012-1312-4

Yang, M., Cheng, B., Song, H., and Chen, X. (2010). "Preparation and electrochemical performance of polyaniline-based carbon nanotubes as electrode materials for supercapacitor," *Electrochim. Acta* 55(23), 7021-7027. DOI: 10.1016/j.electacta.2010.06.077

Yin, J. B., Xia, X., Xiang, L. Q., and Zhao, X. P. (2010). "Conductivity and polarization of carbonaceous nanotubes derived from polyaniline nanotubes and their electrorheology when dispersed in silicone oil," *Carbon* 48(10), 2958-2967. DOI: 10.1016/j.carbon.2010.04.035

Yuan, D. S., Zhou, T. X., Zhou, S. L., Zou, W. J., Mo, S. S., and Xia, N. N. (2011). "Nitrogen enriched carbon nanowires from the direct carbonization of polyaniline nanowires and its electrochemical properties," *Electrochem. Commun.* 13(3), 242-246. DOI: 10.1016/j.elecom.2010.12.023

Zhang, L. L., Zhao, X., Ji, H. X., Stoller, M. D., Lai, L. F., Murali, S., McDonnell, S., Cleveger, B., Wallace, R. M., and Ruoff, R. S. (2012). "Nitrogen doping of graphene and its effect on quantum capacitance, and a new insight on the enhanced capacitance of N-doped carbon," *Energy and Environmental Science* 5(11), 9618-9625.

Zhang, M. Y., Jin, X. J., and Wu, Y. (2013). "Preparation of high performance activated carbon electrode from waste fibreboard for electric double layer capacitor by KOH activation," *Wood Res.* 58(1), 81-90.

Article submitted: September 11, 2014; Peer review completed: May 29, 2015; Revised version received and accepted: July 2, 2015; Published: July 21, 2015.
DOI: 10.15376/biores.10.3.5586-5595